



## OPEN ACCESS

## EDITED BY

Na Li,  
Hainan Medical University,  
China

## REVIEWED BY

Duc-Cuong Bui,  
University of Texas Medical Branch at  
Galveston, United States  
Yong Zhang,  
University of Massachusetts Amherst,  
United States

## \*CORRESPONDENCE

Li Wang  
wli99@jlu.edu.cn

## SPECIALTY SECTION

This article was submitted to  
Infectious Agents and Disease,  
a section of the journal  
Frontiers in Microbiology

RECEIVED 22 September 2022

ACCEPTED 04 November 2022

PUBLISHED 28 November 2022

## CITATION

Zhao B, He D, Gao S, Zhang Y and  
Wang L (2022) Hypothetical protein  
FoDbp40 influences the growth and  
virulence of *Fusarium oxysporum* by  
regulating the expression of isocitrate lyase.  
*Front. Microbiol.* 13:1050637.  
doi: 10.3389/fmicb.2022.1050637

## COPYRIGHT

© 2022 Zhao, He, Gao, Zhang and Wang.  
This is an open-access article distributed  
under the terms of the [Creative Commons  
Attribution License \(CC BY\)](https://creativecommons.org/licenses/by/4.0/). The use,  
distribution or reproduction in other  
forums is permitted, provided the original  
author(s) and the copyright owner(s) are  
credited and that the original publication in  
this journal is cited, in accordance with  
accepted academic practice. No use,  
distribution or reproduction is permitted  
which does not comply with these terms.

# Hypothetical protein FoDbp40 influences the growth and virulence of *Fusarium oxysporum* by regulating the expression of isocitrate lyase

Busi Zhao<sup>1</sup>, Dan He<sup>1</sup>, Song Gao<sup>2</sup>, Yan Zhang<sup>1</sup> and Li Wang<sup>1\*</sup>

<sup>1</sup>Department of Pathogenobiology, Jilin University Mycology Research Center, Key Laboratory of Zoonosis Research, Ministry of Education, College of Basic Medical Sciences, Jilin University, Changchun, China, <sup>2</sup>Beijing ZhongKaiTianCheng Bio-technology Co. Ltd., Beijing, China

Fungal growth is closely related to virulence. Finding the key genes and pathways that regulate growth can help elucidate the regulatory mechanisms of fungal growth and virulence in efforts to locate new drug targets. *Fusarium oxysporum* is an important plant pathogen and human opportunistic pathogen that has research value in agricultural and medicinal fields. A mutant of *F. oxysporum* with reduced growth was obtained by *Agrobacterium tumefaciens*-mediated transformation, the transferred DNA (T-DNA) interrupted gene in this mutant coded a hypothetical protein that we named FoDbp40. FoDbp40 has an unknown function, but we chose to explore its possible functions as it may play a role in fungal growth regulatory mechanisms. Results showed that *F. oxysporum* growth and virulence decreased after FoDbp40 deletion. FOXG\_05529 (NCBI Gene ID, isocitrate lyase, ICL) was identified as a key gene that involved in the reduced growth of this mutant. Deletion of FoDbp40 results in a decrease of more than 80% in ICL expression and activity, succinate level, and energy level, plus a decrease in phosphorylated mammalian target of rapamycin level and an increase in phosphorylated 5'-adenosine monophosphate activated protein kinase level. In summary, our study found that the FoDbp40 regulates the expression of ICL at a transcriptional level and affects energy levels and downstream related pathways, thereby regulating the growth and virulence of *F. oxysporum*.

## KEYWORDS

*Fusarium oxysporum*, CCCH-type zinc finger, ICL, growth, AMPK/mTOR

## Introduction

*Fusarium* species belong to a large genus of filamentous fungi which can infect plants and humans. In 2022, *Fusarium* species were incorporated in High Priority Group of the WHO fungal priority pathogens list (WHO, 2022). *Fusarium oxysporum* can infect cotton, rice, wheat, and other crops, causing diseases including cotton wilt, crown rot in cereal

crops, and head blight in wheat. The fungus seriously affects food safety and causes huge economic loss (Kazan and Gardiner, 2018; Melotto et al., 2020; Zhu et al., 2021). *Fusarium* species are also important opportunistic pathogens in humans, mainly causing corneal infection (keratitis; Alkatan and Al-Essa, 2019), but it can also cause invasive and disseminated infection in immunocompromised people, posing threats to human health (Nucci and Anaissie, 2007; Muraosa et al., 2017).

Fungi virulence is closely related to growth. The cell wall is an essential structure for fungal growth, and some components of cell wall, such as  $\beta$ -1,3-glucans, can participate in activating host immune response and affect virulence in *Aspergillus fumigatus* (Chotirmall et al., 2014). In *Cryptococcus neoformans*, a microtubule-associated CAP-glycine protein (Cgp1) can promote the production of capsules, thereby enhancing virulence (Wang et al., 2018). In *Aspergillus fumigatus*, *Beauveria bassiana*, and *Fusarium graminearum*, strains with slowed growth and sporulation were found to have lower virulence (Paisley et al., 2005; Safavi et al., 2007; Wang et al., 2021). Therefore, studying and finding key regulatory factors, mechanisms, and pathways that regulate fungal growth is crucial to understanding the fungal growth profile, finding new drug targets, and fungal prevention and control methodologies.

Hypothetical proteins are proteins predicted to be expressed from an open reading frame, but with unknown function. Presently, scores of hypothetical proteins exist in the genomes of various animals, plants, fungi, and microorganisms, potentially involving diverse biological processes, including gene expression and protein folding, as well as various life functions, such as host-pathogen interactions and drug tolerance (Wang et al., 2012; Uddin et al., 2019; Pranavathiyani et al., 2020). Hypothetical proteins that regulate growth and virulence have been found in the bacteria *Chlamydia trachomatis* and fungi *Magnaporthe grisea*, among many others (Chen et al., 2006; Lin et al., 2021).

The glyoxylate metabolism pathway is an anabolic variation of the TCA cycle that occurs in most other organisms and converts isocitrate to glyoxylate and succinate. It plays an important role in the growth, pathogenesis, and stress tolerance of fungi such as yeast and *Fusarium* species (Park et al., 2016; Vico et al., 2021). ICL is a key enzyme in the glyoxylate metabolism pathway, responsible for catalyzing the synthesis of succinate, thereby regulating carbon metabolism and ATP synthesis (Gengenbacher et al., 2010; Selinski and Scheibe, 2014). ICL is not present in human and is, therefore, a potential therapeutic target against fungal infection (Bhusal et al., 2017).

Nucleic acid-binding proteins can bind to specific sequences of DNA or RNA and are involved in the transcriptional regulation of cellular processes, such as DNA damage repair and gene expression (Andres et al., 2019; Bartas et al., 2021). Zinc finger proteins are the most abundant class of transcription factors in eukaryotic genomes. These proteins can bind to DNA or RNA, even protein to regulate transcription and play an important role in many life processes (Corkins et al., 2013; Zou et al., 2018).

According to protein sequence, fold, and function, zinc finger proteins can be divided into over 20 primary types, such as  $C_2H_2$ , CCHC, CCCH and so on. Current research mainly focuses on  $C_2H_2$  type zinc finger proteins (Interpro IPR036236), which have the zinc ion coordinated by two cysteine and two histidine residues. CCCH-type zinc finger proteins have a zinc ion coordinated by three cysteines and a single histidine (C-x8-C-x5-C-x3-H; Interpro IPR036855) and account for about 0.8% of zinc finger proteins (Berg and Shi, 1996), but have seldom been reported in fungi. CCCH zinc finger proteins are known as RNA-binding proteins and associated with post-transcriptional regulation of mRNA (Fu and Blakeshear, 2017). In addition to its role in RNA metabolism, recent studies demonstrated that CCCH zinc finger proteins also modulate transcription (Zou et al., 2018; Wang et al., 2022). A RNA-binding CCCH zinc finger protein Zc3h10 was also proved to activate UCP1 promoter by binding to a distal upstream region (Yi et al., 2019).

In this study, a mutant of *F. oxysporum* with reduced growth was obtained by *Agrobacterium tumefaciens*-mediated transformation (ATMT), in which the expression of main genes involved in glyoxylate metabolism pathway were down-regulated. The T-DNA interrupted gene FOXG\_12762 encodes a hypothetical protein containing CCCH-type zinc finger--FoDbp40 [Fo for *F. oxysporum*, Dbp for DNA binding protein, 40 (kDa) for the calculated molecular mass]. The regulation of the expression of ICL by FoDbp40 was elucidated, and the influence of FoDbp40 on the growth and virulence of *F. oxysporum* was discussed.

## Materials and methods

### Construction of random insertion *Fusarium oxysporum* mutants

Wild type *F. oxysporum* JLCC31768 and *Agrobacterium tumefaciens* AgrN (containing plasmid pXEN carrying neomycin and kanamycin resistance tags[*neo*]) were used to generate *F. oxysporum* mutants (He et al., 2021). Wild type and AgrN (Table 1) were preserved at and obtained from the Jilin University Mycology Research Center (Jilin, China).

ATMT of *F. oxysporum* was performed as described previously to obtain mutants with single-strand transferred DNA (T-DNA) inserts (He et al., 2021). The DNA of randomly selected mutants containing the *neo* gene was isolated and amplified using DNA extraction kits (Beyotim, Shanghai, China) and specific *neoF* and *neoR* primers (He et al., 2021). The products were then sequenced by Comate Bioscience Co., Ltd. (Jilin, China) to confirm whether T-DNA was inserted into the *F. oxysporum* genome.

### Analysis of T-DNA interrupted gene

Sequences flanking the inserted T-DNA were amplified by touchdown thermal asymmetric interlaced polymerase chain

TABLE 1 Strains used in this study.

Strain name	Information
WT	Wild type of <i>Fusarium oxysporum</i> JLCC31768, which was obtained from the Jilin University Mycology Research Center (He et al., 2021)
FOM312	T-DNA inserted mutant with reduced growth and virulence (obtained in this study)
$\Delta$ 12762	Deleted FOXG_12762 from wild type (obtained in this study)
C12762	Complemented FOXG_12762 to $\Delta$ 12762 (obtained in this study, EGFP contained)
AgrN	<i>Agrobacterium tumefaciens</i> containing pXEN, which was obtained from the Jilin University Mycology Research Center (He et al., 2021)

reaction (TAIL-PCR) using previously described primers (Gao et al., 2016). The products were sequenced (Comate Bioscience Co., Ltd. Jilin, China) and aligned against the *F. oxysporum* f. sp. *lycopersici* genome (GCF\_000149955.1) using the Basic Local Alignment Search Tool (BLAST<sup>1</sup>) to determine the insertion sites (Lorenzini and Zapparoli, 2019). Bioinformatic analysis for nuclear localization signals was performed by NLStradamus program (Cheng et al., 2019; <http://www.moseslab.csb.utoronto.ca/software/>).

## Construction of the FoDbp40 deletion and complementation strain

We based the method for constructing the targeted knockout of FoDbp40 on homologous genetic recombination by ATMT, with the *neo* marker gene replacing the target gene (He et al., 2021). Primers used are listed in Supplementary Table S2.

Our complementation strain was constructed according to methods described earlier (Roth and Chilvers, 2019). The FoDbp40 open reading frame and its own terminator region were amplified separately. To visualize the localization of FoDbp40 in *F. oxysporum*, the enhanced green fluorescent protein (EGFP) open reading frame was amplified from pEGFP-N3 by PCR. The resulting three DNA fragments were ligated using a One Step Cloning kit (Vazyme, Nanjing, China) and the resulting construct was transformed into protoplasts to create the deletion mutant we named  $\Delta$ 12762. The verification of the deletion and complementation were completed by PCR and observed phenotype. Primers used for all reactions are listed in Table 2. Graphs showing mechanism of the methods were also provided in Supplementary Figures S1, S2.

1 <https://blast.ncbi.nlm.nih.gov/Blast.cgi>

## Growth analysis and microscopic examination

*Fusarium oxysporum* was grown on potato dextrose agar (PDA) for 5 days at 25°C for growth analysis. The conidia were washed down with sterile 0.85% saline containing approximately 1%—Tween<sup>®</sup> 20 and diluted to  $1 \times 10^5$  CFU/ml. Then 2  $\mu$ l of the suspension was dripped onto PDA plates and grown for 5 days at 25°C. Conidia were collected from 5-day-old cultures on PDA. The quantification for each strain was performed in triplicate. Each plate was washed three times with sterile 0.85% saline containing approximately 1%—Tween<sup>®</sup> 20 and the conidia suspension were adjusted to appropriate volume.

Slide cultures were prepared and then examined with microscope after lactophenol cotton blue staining. To visualize the localization of FoDbp40, the slide cultures were stained with 10  $\mu$ g/ml 4',6-diamidino-2-phenylindole (DAPI; Beyotime, Jiangsu, China) for nuclei staining, and then examined with a BX53 microscope (Evident Olympus, Tokyo, Japan).

## Virulence assay

Human corneal epithelial cells (HCEC) were purchased from BeNa culture collection (Jiangsu, China), maintained in Minimum Essential Medium (MEM; XP Biomed Ltd., Shanghai, China) supplemented with 10% heat-inactivated fetal bovine serum (FBS; Gibco, New York, NY, USA) and cultured in 60 ml flasks kept at 37°C in a humidified incubator containing 5% CO<sub>2</sub>.

For *in vitro* cytotoxicity assay, the cultured HCEC were co-cultured with *F. oxysporum* conidia for 24 h (Kolar et al., 2017) in 96-well plates ( $1 \times 10^4$  cells/well), then the lactate dehydrogenase (LDH) released from the cultured HCEC was measured using a lactate dehydrogenase cytotoxicity assay kit (Beyotime, Jiangsu, China; Jin et al., 2007).

An *in vivo* virulence assay was performed with AB strain zebrafish (ZFIN ID: ZDB-GENO-960809-7) as previously described (Laanto et al., 2012). Briefly, zebrafish (three-day post-fertilization) were infected with the *F. oxysporum* conidia by bathing. The fish were individually challenged with  $1 \times 10^4$  CFU/ml conidia, and survival was recorded every 12 h. All the experiments in this study were approved by the animal ethics committee of Jilin University.

## Analysis of gene expression by RT-qPCR

The RNA extraction and construction of cDNA libraries was performed as described previously (He et al., 2021; Wei et al., 2022). Conidia of *F. oxysporum* ( $1 \times 10^6$  CFU) were added to PDB medium and incubated for 24 h. The mycelia were collected and ground to a powder in liquid nitrogen. Total RNA was extracted from the ground material using RNAiso Plus

TABLE 2 Primers used for the vector construction.

Name	Sequence	
12762LF	GATCTTCACTAGTGGGAATTCAGGGCCGCAACGGAAAC	PCR primers for the construction of the gene deletion
12762LR	AGCTCGAATTGCAAGGAGGGAGCGTCAAAGAA	
12762RF	CAGAATAAAGTTTGTAGGTCTGGTGGTGGT	
12762RR	CAGGTCGACTCTAGAGGATCCACCCGTTGCAGTCAAAGCC	
12762NF	CCCTCCTTGCAATTTCGAGCTCGGTACCCAG	
12762NR	GGACCTCAAACTTATTCTGTCTTTTATTGCGGTCCC	
12762p-F	gaccatgattacccaagcttGCTGAGAAGGACAGGCCG	PCR primers for the construction of the complementation vector
12762p-R	ttacccttctgggagcatGATGGGCAGTTGGTGGCG	
12762+e-F	ATGCCTCCCAAGAAGGGTAAG	
12762+e-R	cTTACTTGTACAGCTCGTCCATGC	
12F	CCGCTAGCGCTACCGACTCAGATCTATGCCTCCCAAGAAGGGTAAGGAGG	PCR primers for construction of the vector for Luciferase reporter assay
12R	GCGATGGATCCCGGGCCCGCGCCGCTGCCGCCCGCCGCTGCCGCCCGCCAGATCCGGTTGCTGTCTCAGCTA	
05529proF	ctggcctaactggccggtaccCACAGAGGAAGCAGAGCGAATT	PCR primers for construction of the vector for Luciferase reporter assay
05529proR	cagtaccggattccaagcttTCTAGCTCGGCTTCCACCG	
XF	CGAGTGGTGATTTTGTGCCG	PCR primers for identification
XR	AAACTGAAGGCGGAAACGA	
TRF	GCCTATGAAAAACGCCAGC	
TRR	CAACTGTGGGAAGGGCGA	

According to the instruction, some primers for vector construction was design with a cohesive end which was wrote as normal letter.

TABLE 3 Primers used for qPCR.

Name	Sequence
Fu18SF	CGCCAGAGGACCCCTAAAC
Fu18SR	ATCGATGCCAGAACCAAGAGA
05529F	GAAGGAGGTTGAGGCTGTCAAG
05529R	CGTAGGTGTAGCTGGCATCTC
10116F	AGCTCTGATGGTCCCTGGAT
10116R	TGCGTTTACAACCAGAAAGCAG
01304F	ACCTAAGCGAAACGGGTCTG
01304R	ATTGAATGCCGTGGTCTCGT
10419F	CGCACTCGACTACATTCCCA
10419R	GTGCAGAGATGCCCTTGACT
12762F	GTCAAAGAAGGCAACCAGC
12762R	TGGTCTTCAGGACGAATCCAG

The number in the primer name is the same as the gene ID. For example, 12762F is used for amplification of FOXG\_12762. All primers in this table were designed with a T<sub>m</sub> of 60°C.

(TaKaRa, Japan). Real-time, quantitative PCR (RT-qPCR) analysis was performed with a SYBR Green master mix (Monad, Shanghai, China) and the ABI QuantStudio 3 PCR system (Applied Biosystems, Waltham, MA, USA). Relative expression levels of the genes were calculated using the threshold cycle ( $2^{-\Delta\Delta CT}$  also known as 2<sup>2DDCT</sup>) method (Livak and Schmittgen, 2001). Gene expression levels were normalized against the expression of the 18S rRNA housekeeping gene (Table 3). Details regarding the relevant primers are provided in Supplementary Table S3.

## ICL activity assay and measurement of succinic acid

Isocitrate lyase (ICL) activity was measured with an ICL activity assay kit of (Comin Corporation, Suzhou, China). After 24h cultured in PDB, mycelia were collected and ground to a powder in liquid nitrogen. The mycelium powder was homogenized in 200  $\mu$ l distilled water, and then centrifuged at 12,000 g at 4°C for 15 min. The supernatant was treated according to manufacturer's protocol, and the absorbance of the samples at 340 nm was detected using a spectrophotometer (Agilent Biotek, Santa Clara, CA, USA). The ICL activity was expressed as nmol/min/g.

Succinic acid was detected by high performance liquid chromatography (HPLC). A RIGOL (Suzhou, China) L3000 chromatograph and RIGOL C18 reversed-phase column (250 mm  $\times$  4.6 mm, 5  $\mu$ m) were employed. The mobile phase was prepared as follows: 1.56 g of sodium dihydrogen phosphate was dissolved in 800 ml of water, then 16 ml of methanol was added and the pH was adjusted to 4–5 with a phosphoric acid solution; 10  $\mu$ l of samples were loaded; the flow rate was 0.8 ml/min; the column temperature was 30°C; the sampling time was 30 min at 214 nm UV.

## Luciferase reporter assay

The FOXG\_12762 (NCBI Gene ID, mRNA accession XM\_018392621) CDS region was inserted into the pEGFP-N3 (Takara Clontech, Kyoto, Japan) multiple cloning site (MCS) to

construct our FoDbp40-EGFP fusion protein expression vector (vector 1). The FOXG\_05529 (NCBI Gene ID, isocitrate lyase) promoter region (regarded as  $-2,000$  to  $+200$ ) was inserted upstream of *luc2* in pGL4.10 (Promega, Madison, WI, USA) to construct our 05529pro-*luc2* expression vector (vector 2).

Human embryonic kidney 293 (HEK-293) cells were maintained in high-glucose, GlutaMAX™ Dulbecco's Modified Eagle Medium (DMEM; Thermo Fischer Scientific, Waltham, MA, USA) supplemented with 10% heat-inactivated FBS (Gibco Thermo Fischer Scientific, Waltham, MA, USA) and cultured in 60 ml flasks kept at 37°C in a humidified incubator containing 5% CO<sub>2</sub>. For transfections, HEK-293 cells were grown in FBS-containing medium in six-well plates until they reached 70% confluency. The transfection solution was prepared by mixing vector 1, pGL4.10 (Promega, Madison, WI, USA) basic vector or vector 2, pGL4.74 (Promega, Madison, WI, USA) containing the luciferase reporter gene *hRluc* for internal reference, Lipofectamine® 3,000 (Invitrogen Thermo Fischer Scientific, Waltham, MA, USA). Twenty-four hours later fluorescence from the enhanced green fluorescent protein (EGFP) was examined under an Olympus Model IX71 fluorescent microscope (Evident Olympus, Tokyo, Japan) to judge whether the FoDbp40-EGFP fusion protein was successfully expressed. Firefly and *Renilla* luminescence were tested using a Dual-Glo® Luciferase Assay System (Promega, Madison, WI, USA)<sup>2</sup> with a spectrophotometer (Agilent Biotek, Santa Clara, CA, USA). The relative expression of *luc2* was expressed as the ratio of firefly to *Renilla* luminescence signal. HEK-293 cells and pEGFP-N3 were obtained from Jilin University Mycology Research Center (Jilin, China). Primers used are provided in [Supplementary Table S2](#).

## ATP level assay

Mycelia ATP levels were determined using an ATP assay kit (Beyotime, Jiangsu, China) according to the manufacturer's instructions. After 24 h cultured in PDB, 100 mg of mycelia were collected and ground into powder in liquid nitrogen, the powder was homogenized in a lysis buffer and then centrifuged at 12,000 g for 5 min at 4°C. The supernatant was mixed with the working solution. The mixture was put into microwell plates and fluorescence intensity was measured with a spectrophotometer (Agilent Biotek, Santa Clara, CA, USA). The ATP levels were expressed as nmol/g.

## Western blot analysis

The western blot method was performed as previously described (Li et al., 2010).  $1 \times 10^6$  conidia were inoculated in 50 ml of potato dextrose broth (PDB) and cultured with shaking at 28°C for 24 h. Mycelia were harvested and ground into powder in liquid nitrogen, then suspended in radioimmunoprecipitation assay (RIPA) buffer

containing 1 mM phenylmethylsulfonyl fluoride (PMSF). 20 µg of sample was loaded in each lane of a 10% SDS-PAGE gel. After electrophoresis, the samples were transferred to a polyvinylidene fluoride (PVDF) membrane. The membrane was then blocked with Tris-buffered saline with 0.1% Tween® 20 detergent (TBST) buffer containing 5% milk. After incubation with primary and secondary antibodies, blots were developed using enhanced chemiluminescence (ECL) western blot detection reagent (Bio-Rad, Hercules, California, USA) and images were acquired using a Tanon 4,200 Chemiluminescence Imaging System (Tanon, Shanghai, China). Antibodies used (anti-Actin, anti-AMPK alpha-1, anti-Phospho-AMPK alpha-1, mTOR, and anti-Phospho-mTOR) were purchased from Invitrogen (Thermo Fischer Scientific, Waltham, MA, USA).

## Statistical analysis

All statistical analyses were performed using GraphPad Prism software version 6 (Dotmatics, San Diego, CA, USA). One-way analysis of variance followed by *t*-test was used for comparisons between the groups.  $p < 0.05$  was considered to indicate a statistically significant difference.

The flow chart of present study was provided in supplementary materials ([Supplementary Figure S3](#)).

## Results

### Screening of *Fusarium oxysporum* mutants with reduced growth

Mutants of *F. oxysporum* were obtained by random insertion of T-DNA into the *F. oxysporum* genome using ATMT. A single specific amplicon can be amplified from all mutants ([Supplementary Figure S4](#)). The sequenced fragment was 100% identical to the *neo* gene, which proved that the T-DNA was successfully inserted into the *F. oxysporum* genome.

Mutant strains growth was compared to wild type *F. oxysporum* and FOM312 was identified with significantly reduced radial growth ([Figure 1A](#)). There were also other mutants were screened out with changed phenotype including slowed down growth, mycelial morphology changed, pigment decreased, etc., which were not discussed here.

### Detection of the expression of genes involved in glyoxylate metabolism pathway in FOM312

The expression of four genes related to the glyoxylate metabolism pathway in FOM312 was detected by qPCR ([Figure 2](#)). The results showed that the expression of the four genes was down-regulated, and the expression of ICL was the most down-regulated. ICL is the rate limiting enzyme of the

<sup>2</sup> <https://www.promega.com.cn/products/luciferase-assays/>

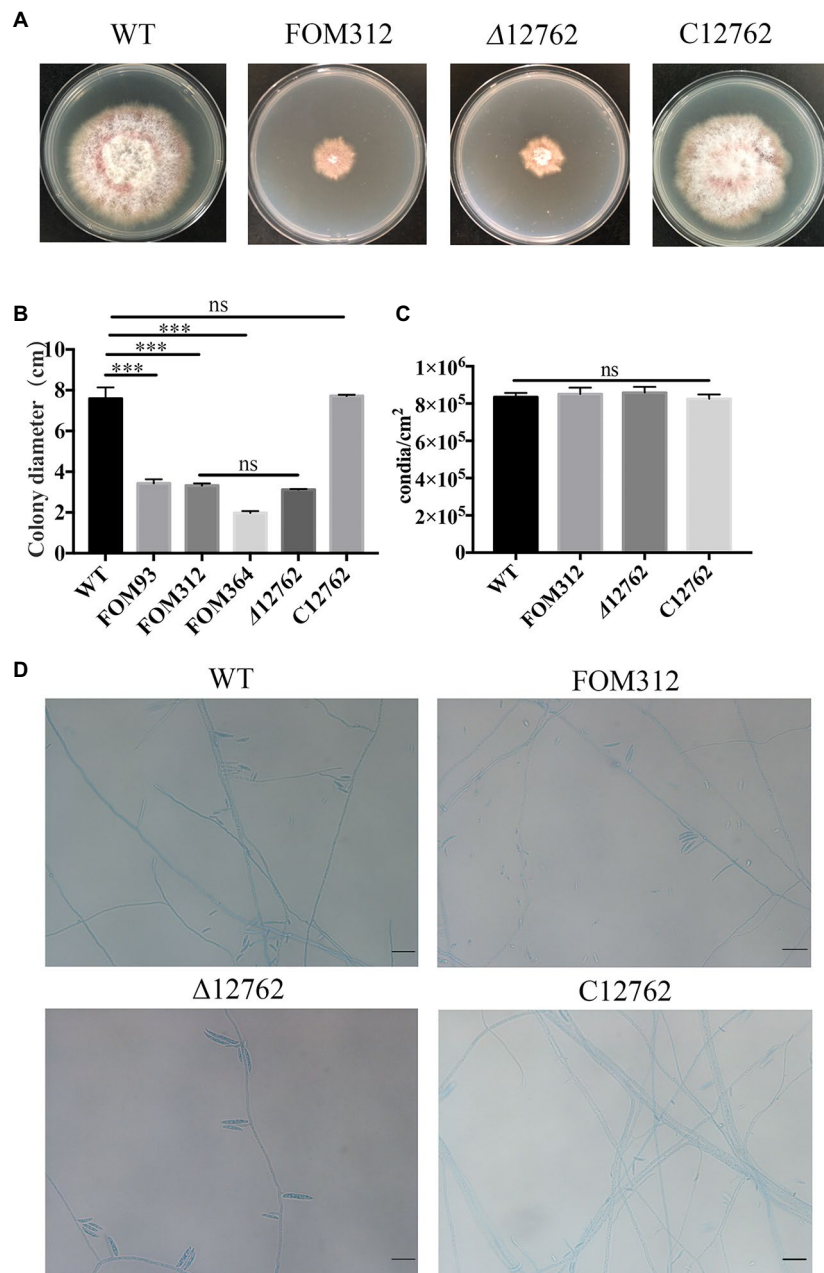


**FIGURE 1**  
**(A)** Radial growth of wild type (WT), FOM312, Δ12762, and C12762. Strains were cultured on PDA medium and incubated at 25°C for 5 days. **(B)** The quantitative data for A (\*\*\*)  $p < 0.001$ . **(C)** Conidial production rate of wild type, FOM312, Δ12762, and C12762. **(D)** The slide culture of wild type, FOM312, Δ12762, and C12762 (bar=25μm). The experiment was repeated three times.

glyoxylate metabolism pathway. Therefore, we speculate that FoDbp40 may affect energy metabolism and the growth of *F. oxysporum* by regulating ICL expression.

### Analysis of T-DNA interrupted gene in the FOM312

T-DNA interrupted genes in FOM312 was verified by sequencing the TAIL-PCR products. The T-DNA in FOM312

inserted into FOXG\_12762, which is located on chromosome 9 and encodes a hypothetical protein.

An amino acid sequence analysis performed with MEGA indicated that similar proteins are produced by other fungal species (Figure 3). FOXG\_12762 encodes a hypothetical protein containing a CCCH zinc finger domain. This hypothetical protein has a high sequence identity (more than 70%) with homologs in common *Fusarium* species such as *F. graminearum* and *F. solani* and filamentous fungi such as *Aspergillus fumigatus* and *Torrubiella hemipterigena*. Sequence identity with other homologs,

such as *Aspergillus nidulans* and *Aspergillus flavus*, is lower (60–70%). The homologs in *Aspergillus fumigatus* (79%), *Colletotrichum incanum* (80%), and *Torrubiella hemipterigena* (81%) are annotated as CCCH zinc finger DNA binding proteins. According to the bioinformatic analysis for nuclear localization signals, there are three sections of the sequence predicted to be nuclear localization signals (Figure 3; Supplementary Figure S5).

### Constructs for gene deletion and mutant complementation of FOXG\_12762

A knockout strain ( $\Delta$ 12762) and complementation strain (C12762) of FOXG\_12762 were constructed. The deletion and complementation were verified by PCR (Supplementary Figures S1, S2). After 5 days of culture at 25°C, the  $\Delta$ 12762 colony was similarly sized to FOM312. The C12762 colony was similar in size to the wild type (Figures 1A,B). The expression of FOXG\_12762 was significantly decreased after interrupted by T-DNA in FOM312, and was similar with wild

type in C12762, while no signal was detected in  $\Delta$ 12762, which proved the successful deletion and complementation (Figure 4A). Based on the microscopic phenotype, the hyphae in the FOM312 and  $\Delta$ 12762 reduced compared with wild-type and C12762 (Figure 1D). Nevertheless, there was no much difference in conidial production between them (Figure 1C).

### Analysis of ICL expression regulation by FOXG\_12762

The expression level of FOXG\_05529 and ICL activity were detected and results show that the mRNA level of FOXG\_05529 and ICL activity in  $\Delta$ 12762 and FOM312 decreased compared with wild type and C12762 (Figures 4B,C). HPLC results show that the level of succinic acid in FOM312 and  $\Delta$ 12762 also decreased, and the level of succinic acid in C12762 was close to that of wild type (Figure 4D). These results indicate that FoDbp40 can regulate the expression level and activity of ICL and affect the growth of *F. oxysporum*.

FoDbp40 has high sequence identity to various CCCH zinc finger DNA-binding proteins in other fungi. This implies that it may have functions of binding to DNA and regulating transcription. To confirm whether FoDbp40 can regulate the transcription of the ICL-encoding gene FOXG\_05529, the action of FoDbp40 on the promoter region of FOXG\_05529 was investigated using dual luciferase reporter technology. The HEK-293 cells co-transfected with the FoDbp40-EGFP fusion protein expression vector (vector 1) and the 05529pro-luc2 expression vector (vector 2) can produce green fluorescence under 488 nm wavelength excitation, which indicates that the FoDbp40-EGFP fusion protein was successfully expressed in the HEK-293 cells (Figures 5A–C). Compared with the vector 2 transfection group, the luc2 fluorescence signal of the vector 1 and vector 2 co-transfected group was significantly enhanced (Figure 5D). These results indicate that FoDbp40 can act on the FOXG\_05529 promoter region to promote the transcription and expression of downstream genes.

The cellular localization of the FoDbp40-EGFP fusion protein was observed using fluorescence microscopy. Results show that FoDbp40-EGFP is primarily located in the nucleus, as demonstrated by DAPI staining (Figure 6).

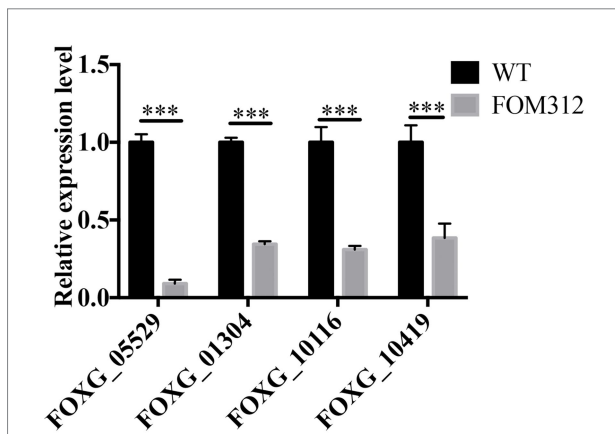


FIGURE 2 The relative expression level of four genes involved in glyoxylate metabolic pathway in FOM312. FOXG\_05529 codes isocitrate lyase; FOXG\_01304 codes 2-methylcitrate synthase; FOXG\_10116 codes a formate/nitrite transporter domain; FOXG\_10419 codes malate dehydrogenase. 18S rRNA was used as normalizing (\*\*p < 0.001). The experiment was repeated three times.

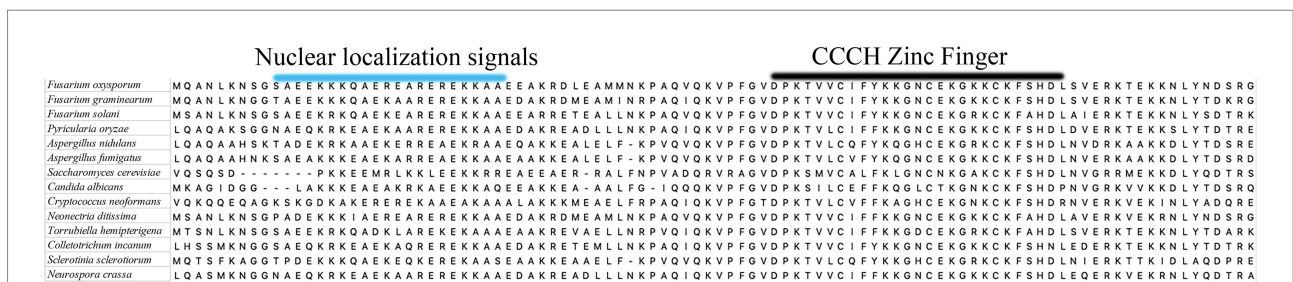
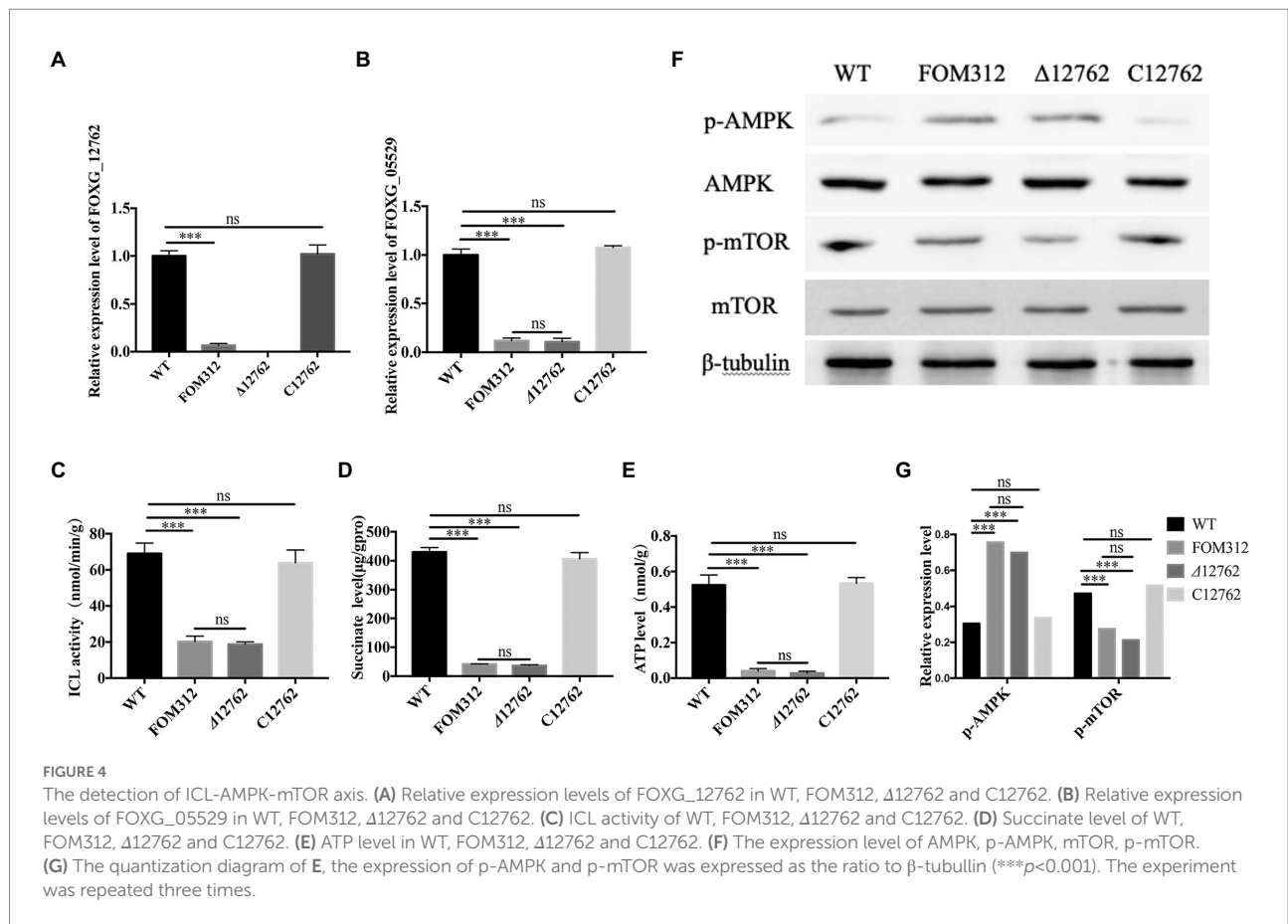


FIGURE 3 A part of the alignment result of amino acid sequences of FOXG\_12762 and its most similar homologs from other fungi.



## FoDbp40 regulates the AMPK/mTOR signaling pathway and energy levels

Considering the activity of ICL in regulating energy metabolism, we detected the ATP levels in wild type, FOM312, Δ12762, and C12762. ATP levels are decreased in the FOM312 and Δ12762 strains compared with the wild type and C12762 strain (Figure 4E). The 5'-adenosine monophosphate activated protein kinase (AMPK) and mammalian target of rapamycin (mTOR) phosphorylation levels were detected by western blot. The results show that the level of phosphorylated-AMPK (p-AMPK) increased and the level of phosphorylated-mTOR (p-mTOR) decreased in Δ12762 and FOM312 compared with wild type and C12762 (Figures 4F,G). These results indicate that the loss of FoDbp40 causes a decrease in ATP levels, which affects the regulation of AMPK/mTOR pathways, thereby causing reduced growth and virulence of *F. oxysporum*.

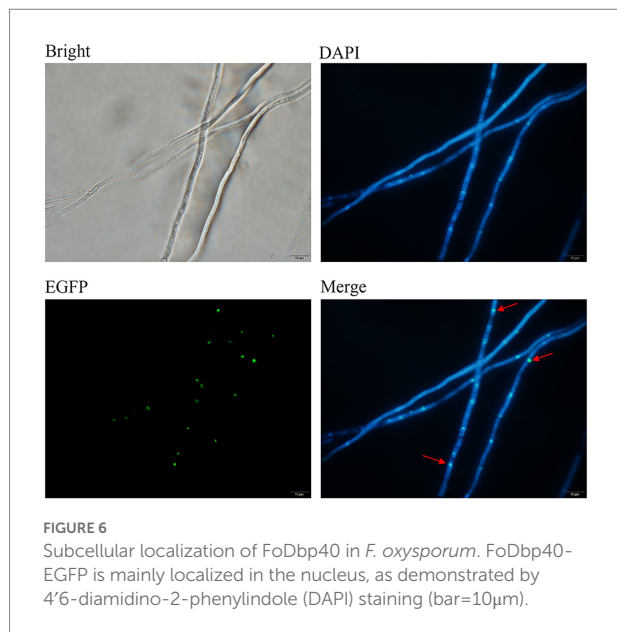
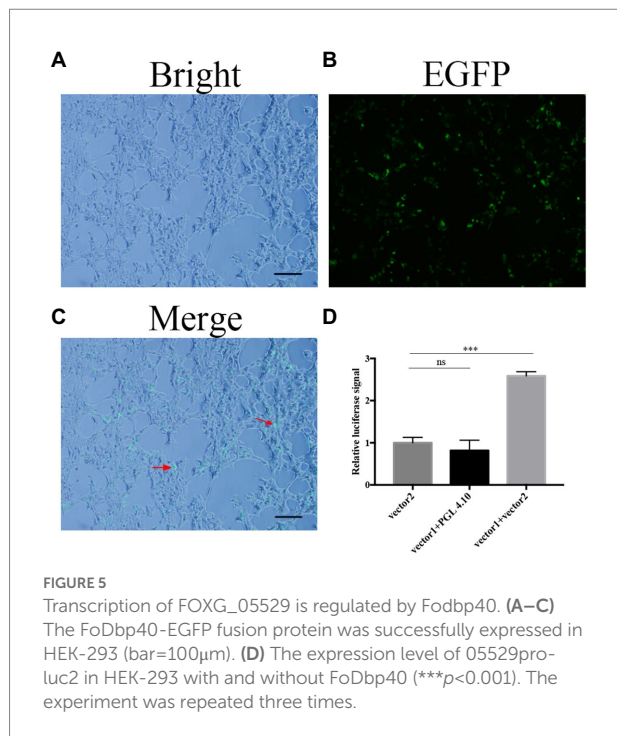
## Deletion of FOXG\_12762 reduced the virulence of *Fusarium oxysporum*

Different concentrations of conidia were co-cultured with HCEC for 24 h, and HCEC cell viability was detected by an

LDH detection kit (Beyotime, Shanghai, China). Results show that FOM312 and Δ12762 ( $1.8 \times 10^6$  CFU/ml for half maximal inhibitory concentration [IC<sub>50</sub>]) have a lower cytotoxicity compared with wild type ( $2.4 \times 10^6$  CFU/ml for IC<sub>50</sub>). This indicates that the deletion of FOXG\_12762 results in decreased *F. oxysporum* virulence in HCEC (Figure 7A).

The IC<sub>50</sub> of wild type with HCEC was  $1.8 \times 10^6$  CFU/ml; therefore, this concentration was selected to stimulate HCEC cells to observe inflammation levels. Results show that the expression levels of IL-1β, IL-6, and TNF-α in HCEC increase after 6 h of stimulation (Figures 7B–D). Compared with the wild type treated group, the levels of inflammatory factors in the FOM312 and Δ12762 treated groups were lower, and the level of inflammatory factors in the C12762 treated group were close to those of the wild type treated group. This indicates that the deletion of FOXG\_12762 can reduce the level of inflammatory response caused by *F. oxysporum*.

Zebrafish were inoculated with  $1 \times 10^4$  CFU/ml conidia to observe survival rates. Results show that the lethality of FOM312 and Δ12762 groups was lower than wild type and C12762, which suggest that the virulence of *F. oxysporum* decreased due to a deficiency of FOXG\_12762 (Figure 7E).



## Discussion

*Fusarium* species are important plant pathogens and human opportunistic pathogens that seriously affect the yield of crops and human health. Fungi growth is closely related to virulence. Exploring the regulatory mechanism of *Fusarium* growth is helpful for the development of new drugs, as well as the prevention and control of *Fusarium* infection. Constructing random mutants of fungi by ATMT is convenient

due to high efficiency, which has been extensively used in numerous fungi to clarify the function of unknown genes (Schmidpeter et al., 2017; de Vallée et al., 2019). We used the ATMT method combined with phenotypic screening to search for key genes in growth and regulatory mechanisms in *F. oxysporum*.

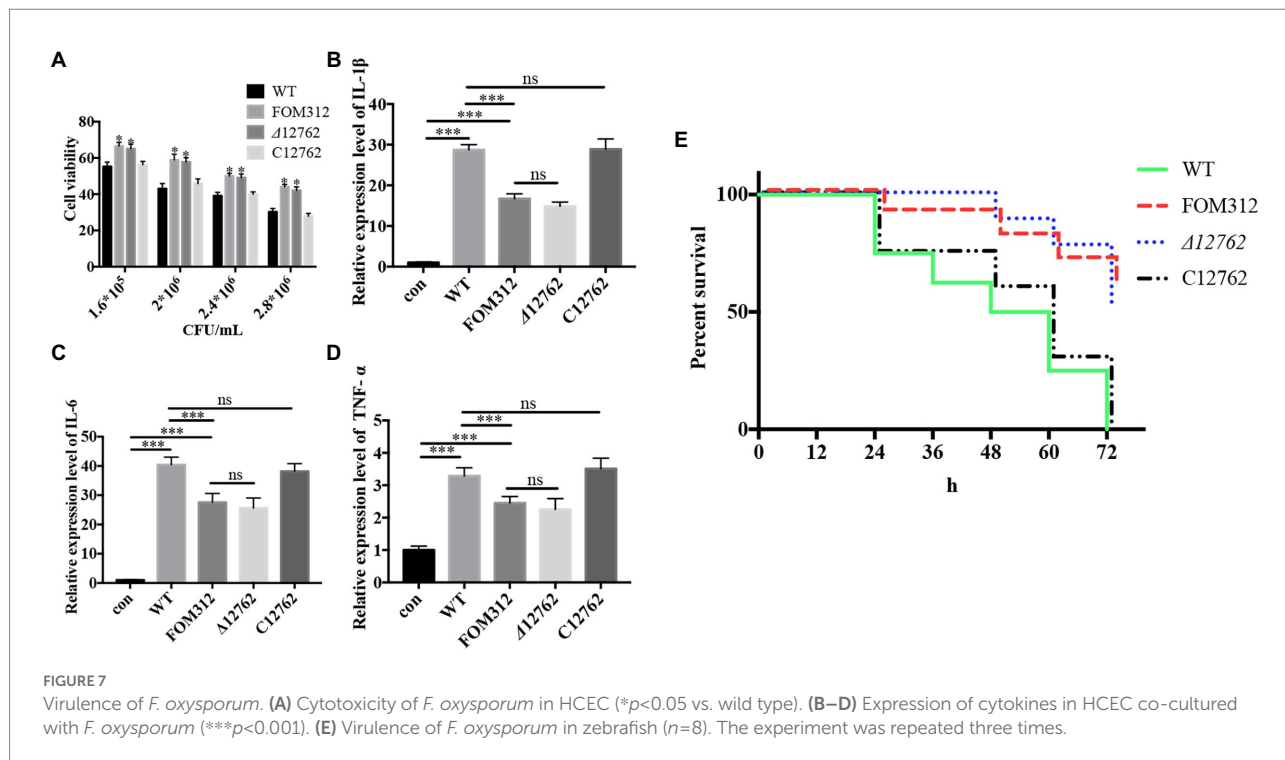
The glyoxylate metabolism pathway plays an important role in the growth, pathogenesis, and stress tolerance of fungi (Park et al., 2016; Vico et al., 2021). Therefore, the expression of four genes related to glyoxylate metabolic pathways were detected. The results showed that the four genes were down-regulated in FOM312 compared with wild type. Among the four genes, the rate limiting enzyme ICL was most down-regulated, so we speculated that the interruption of T-DNA in FOM312 may disturbed the expression of ICL.

In order to investigate the mechanism of regulation of ICL, the function of T-DNA interrupted gene FOXG\_12762 in FOM312 was analyzed. FOXG\_12762 encodes a hypothetical protein that we name FoDbp40. Presently the annotation of hypothetical proteins is primarily through homology search and the identification of conserved domains by sequence alignment algorithms (Ijaq et al., 2015). Our amino acid sequence alignment shows the FoDbp40 protein sequence to contain a CCCH zinc finger domain conserved in several pathogenic fungi (Figure 3). Homologs in other fungi such as *Aspergillus fumigatus* and *Torribiella hemipterigena* are annotated as CCCH zinc finger DNA binding proteins. Although CCCH zinc finger proteins were known as RNA-binding proteins (Fu and Blackshear, 2017), Recent studies showed that CCCH zinc finger proteins also bind to DNA and modulate transcription (Zou et al., 2018; Wang et al., 2022). Therefore, we speculate that FoDbp40 may have the ability to bind target DNA and function in transcriptional regulation.

In this study, we observed the regulatory effect of FoDbp40 on ICL expression (Figure 4) and demonstrated that this regulatory effect is achieved at the transcriptional level by acting on the promoter region of ICL (Figure 5). Additionally, we observed the FoDbp40 protein to localize in the nucleus (Figure 6) in line with the bioinformatic analysis (Supplementary Figure S5), which is similar to other known CCCH zinc finger protein transcription factors, including C3H12 and SAW1 (Wang et al., 2020; Seok et al., 2022). Our results indicate that FoDbp40 is a novel transcriptional regulator that can affect the expression and activity of ICL.

The glyoxylate metabolic pathway saves carbon sources by skipping the step of generating CO<sub>2</sub> in the tricarboxylic acid cycle (TCA) while generating required intermediates. This plays an important role in the regulation of ATP synthesis (Park et al., 2016). The expression and activity of ICL and corresponding succinate levels are decreased after the deletion of FOXG\_12762 (Figure 4). These results demonstrated the regulatory effect of FoDbp40 on ICL and glyoxylate metabolic pathway.

As mentioned above, ICL is a key enzyme in the glyoxylate metabolism pathway, thereby regulating carbon metabolism and



ATP synthesis (Gengenbacher et al., 2010; Selinski and Scheibe, 2014). AMPK, an AMP-dependent protein kinase, is a key molecule in the regulation of biological energy metabolism. Intracellular energy level can regulate the phosphorylation of AMPK, which in turn regulates the Ras, ERK, mTOR, and other related pathways that crosstalk with AMPK, thus affecting cell growth (Hardie, 2014; Grahl et al., 2015). The regulation of growth by the AMPK/mTOR pathways has been reported in yeast (Forte et al., 2019), but has not been reported in *Fusarium* species.

The affect of FoDbp40 on the level of ATP and AMPK/mTOR pathway which involved in the growth regulation was analyzed at next. The results showed that the deletion of FoDbp40 results in a severe decrease of ATP levels in *F. oxysporum* (by more than 80%), while promoting phosphorylation of AMPK and dephosphorylation of mTOR (Figure 4). These results demonstrated the regulatory effects of FoDbp40 on energy metabolism and AMPK/mTOR pathways through the ICL.

*Fusarium* species often cause corneal infection in clinic. Some studies have used HCEC cells to establish *in vitro* model of cornea infection by pathogens such as *Fusarium solani* (Kolar et al., 2017). *F. solani* and *F. oxysporum* both belong to the genus *Fusarium*, which were the most predominant pathogenic *Fusarium* in clinic with similar infection and pathogenic patterns. Therefore, HCEC cells were used in this study to evaluate the virulence of *F. oxysporum*.

The pathogenesis of keratitis is often accompanied by an inflammatory response related to its prognosis (Matsumoto et al., 2005). Pattern recognition receptors on cell surfaces can regulate the expression of inflammatory cytokines after recognizing pathogens. These include IL-1 $\beta$ , IL-6, and TNF- $\alpha$ ; all cause inflammatory response (Yu et al., 2017). After the deletion of

FOXG\_12762, the cytotoxicity of *F. oxysporum* conidia in HCEC was attenuated, and the expression levels of pro-inflammatory cytokines in infectious keratitis decreased (Figure 7).

Dananjaya et al. (2017) have used zebrafish to evaluate the virulence of *F. oxysporum*. Considering that *F. oxysporum* often cause superficial infection in clinic, we established a model of *F. oxysporum* infection in zebrafish with the method of bathing referring to the virulence assay of Laanto et al. (2012) proceeded with *Flavobacterium columnare*. The results showed that there was a stable killing effect on zebrafish infected with *F. oxysporum*. Therefore, we believe that this model is suitable for evaluating the virulence of pathogenic fungi in superficial infection. In this study, the deletion of FOXG\_12762 results in attenuated virulence of *F. oxysporum* in zebrafish (Figure 7). These results indicate that FOXG\_12762 plays an important role in regulating *F. oxysporum* virulence.

In summary, our findings demonstrate that the gene encoding ICL is a key component affecting the growth of *F. oxysporum*. Furthermore, the putative protein FoDbp40 can regulate the expression of ICL at the transcriptional level, thereby affecting the level of ATP and the AMPK/mTOR pathways, and consequently regulate *F. oxysporum* growth and virulence. ICL and FoDbp40 have potential as new targets in the development of antifungal drugs.

## Data availability statement

The original contributions presented in the study are included in the article/Supplementary material, further inquiries can be directed to the corresponding author.

## Ethics statement

The animal study was reviewed and approved by the animal ethics committee of Jilin University (Jilin University, Changchun, China).

## Author contributions

DH and LW: conceptualization and design. BZ and YZ: methodology and experiments. SG: data analysis. BZ and DH: original manuscript. LW: review and editing. All authors contributed to the article and approved the submitted version.

## Funding

This study was supported by grants from the National Natural Science Foundation of China (81772162 and U1704283) and the Foundation of Jilin Education Committee (JJKH20211150KJ).

## Acknowledgments

We thank all staff of our research center for helpful discussions. We also thank Steven M. Thompson from Liwen Bianji (Edanz; [www.liwenbianji.cn/](http://www.liwenbianji.cn/)), for editing the English text of a draft of this manuscript.

## Conflict of interest

SG was employed by Beijing ZhongKaiTianCheng Bio-technonogy Co. Ltd., Beijing, China.

The remaining authors declare that the research was conducted in the absence of any commercial or financial

## References

- Alkatan, H. M., and Al-Essa, R. S. (2019). Challenges in the diagnosis of microbial Keratitis: a detailed review with update and general guidelines. *Saudi J. Ophthalmol.* 33, 268–276. doi: 10.1016/j.sjopt.2019.09.002
- Andres, S. N., Li, Z. M., Erie, D. A., and Scott Williams, R. (2019). Ctp 1 protein-DNA filaments promote DNA bridging and DNA double-strand break repair. *J. Biol. Chem.* 294, 3312–3320. doi: 10.1074/jbc.RA118.006759
- Bartas, M., Červeň, J., Guziurová, S., Slychko, K., and Pečinka, P. (2021). Amino acid composition in various types of nucleic acid-binding proteins. *Int. J. Mol. Sci.* 22:922. doi: 10.3390/ijms22020922
- Berg, J. M., and Shi, Y. (1996). The galvanization of biology: a growing appreciation for the roles of zinc. *Science* 271, 1081–1085. doi: 10.1126/science.271.5252.1081
- Bhusal, R. P., Bashiri, G., Kwai, B. X. C., Sperry, J., and Leung, I. K. H. (2017). Targeting isocitrate lyase for the treatment of latent tuberculosis. *Drug Discov. Today* 22, 1008–1016. doi: 10.1016/j.drudis.2017.04.012
- Chen, C., Chen, D., Sharma, J., Cheng, W., Zhong, Y., Liu, K., et al. (2006). The hypothetical protein CT813 is localized in the chlamydia trachomatis inclusion membrane and is immunogenic in women urogenitally infected with *C. trachomatis*. *Infect. Immun.* 74, 4826–4840. doi: 10.1128/IAI.00081-06
- Cheng, J. H., Lai, G. H., Lien, Y. Y., Sun, F. C., Hsu, S. L., Chuang, P. C., et al. (2019). Identification of nuclear localization signal and nuclear export signal of VP1 from the chicken anemia virus and effects on VP2 shuttling in cells. *Virology* 16:45. doi: 10.1186/s12985-019-1153-5
- Chotirmall, S. H., Mirkovic, B., Lavelle, G. M., and McElvaney, N. G. (2014). Immuno-evasive Aspergillus virulence factors. *Mycopathologia* 178:363070, 363–370. doi: 10.1007/s11046-014-9768-y
- Corkins, M. E., May, M., Ehrensberger, K. M., Hu, Y. M., Liu, Y. H., Bloor, S. D., et al. (2013). Zinc finger protein Loz1 is required for zinc-responsive regulation of gene expression in fission yeast. *Proc. Natl. Acad. Sci. U. S. A.* 110, 15371–15376. doi: 10.1073/pnas.1300853110
- Dananjaya, S. H. S., Udayangani, R. M. C., Shin, S. Y., Edussuriya, M., Nikapitiya, C., Lee, J., et al. (2017). In vitro and in vivo antifungal efficacy of plant based lawsone against *Fusarium oxysporum* species complex. *Microbiol. Res.* 201, 21–29. doi: 10.1016/j.micres.2017.04.011
- de Vallée, A., Bally, P., Bruel, C., Chandat, L., Choquer, M., Dieryckx, C., et al. (2019). A similar Secretome disturbance as a Hallmark of non-pathogenic Botrytis cinerea ATMT-mutants? *Front. Microbiol.* 10:2829. doi: 10.3389/fmicb.2019.02829

relationships that could be construed as a potential conflict of interest.

## Publisher's note

All claims expressed in this article are solely those of the authors and do not necessarily represent those of their affiliated organizations, or those of the publisher, the editors and the reviewers. Any product that may be evaluated in this article, or claim that may be made by its manufacturer, is not guaranteed or endorsed by the publisher.

## Supplementary material

The Supplementary material for this article can be found online at: <https://www.frontiersin.org/articles/10.3389/fmicb.2022.1050637/full#supplementary-material>

### SUPPLEMENTARY FIGURE S1

(A) Mechanism of the deletion of FOXG\_12762. (B) Amplification of neo fragment from the candidate strains. M, maker; lane 1, wild type; lane 2, pXEN plasmid, 3–5, different candidate strains. (C) Amplification of part of FOXG\_12762 sequence from the candidate strains. M, maker; lane 1, water as blank; lane 2, wild type; lane 3–5, different candidate strains.

### SUPPLEMENTARY FIGURE S2

(A) Mechanism of the complementation of FOXG\_12762. (B) Amplification of FOXG\_12762-EGFP sequence from the candidate strains. M, maker; lane 1, Δ12762; lane 2–4, different candidate strains. A fragment (~4500bp) could be obtained from the candidates.

### SUPPLEMENTARY FIGURE S3

The flow chart of analyzing the function of FoDpb40 on the growth and virulence of *F. oxysporum*.

### SUPPLEMENTARY FIGURE S4

Amplification of neo fragment (~700bp) in some randomly selected mutants. M: Trans 2 K marker; lane1: water as blank; lane2: pXEN plasmid; lane3: wild-type *F. oxysporum*; lane4–16: different mutants.

### SUPPLEMENTARY FIGURE S5

The prediction of nuclear localization signals in FOXG\_12762. Three nuclear localization signals were predicted.

- Forste, G. M., Davie, E., Lie, S., Franz-Wachtel, M., Ovens, A. J., Wang, T., et al. (2019). Import of extracellular ATP in yeast and man modulates AMPK and TORC1 signalling. *J. Cell Sci.* 132:jcs223925. doi: 10.1242/jcs.223925
- Fu, M., and Blakeshear, P. J. (2017). RNA-binding proteins in immune regulation: a focus on CCCH zinc finger proteins. *Nat. Rev. Immunol.* 17, 130–143. doi: 10.1038/nri.2016.129
- Gao, S., He, D., Li, G., Zhang, Y., Lv, H., and Wang, L. (2016). A method for amplification of unknown flanking sequences based on touchdown PCR and suppression-PCR. *Anal. Biochem.* 509, 79–81. doi: 10.1016/j.ab.2016.07.001
- Gengenbacher, M., Rao, S. P. S., Pethe, K., and Dick, T. (2010). Nutrient-starved, non-replicating mycobacterium tuberculosis requires respiration, ATP synthase and isocitrate lyase for maintenance of ATP homeostasis and viability. *Microbiology* 156, 81–87. doi: 10.1099/mic.0.033084-0
- Grahl, N., Demers, E. G., Lindsay, A. K., Harty, C. E., Willger, S. D., Piispanen, A. E., et al. (2015). Mitochondrial activity and Cyr1 are key regulators of Ras1 activation of *C. albicans* virulence pathways. *PLoS Pathog.* 11:e1005133. doi: 10.1371/journal.ppat.1005133
- Hardie, D. G. (2014). AMPK--sensing energy while talking to other signaling pathways. *Cell Metab.* 20, 939–952. doi: 10.1016/j.cmet.2014.09.013
- He, D., Feng, Z., Gao, S., Wei, Y., Han, S., and Wang, L. (2021). Contribution of NADPH-cytochrome P450 reductase to azole resistance in *Fusarium oxysporum*. *Front. Microbiol.* 12:709942. doi: 10.3389/fmicb.2021.709942
- Jjaq, J., Chandrasekharan, M., Poddar, R., Bethi, N., and Sundararajan, V. S. (2015). Annotation and curation of uncharacterized proteins-challenges. *Front. Genet.* 6:119. doi: 10.3389/fgenet.2015.00119
- Jin, X., Qin, Q., Tu, L., Zhou, X., Lin, Y., and Qu, J. (2007). Toll-like receptors (TLRs) expression and function in response to inactivate hyphae of fusarium solani in immortalized human corneal epithelial cells. *Mol. Vis.* 13, 1953–1961. PMID: 17982419. <http://www.molvis.org/molvis/v13/a220/>.
- Kazan, K., and Gardiner, D. M. (2018). Fusarium crown rot caused by *Fusarium pseudograminearum* in cereal crops: recent progress and future prospects. *Mol. Plant Pathol.* 19, 1547–1562. doi: 10.1111/mpp.12639
- Kolar, S. S., Baidouri, H., and McDermott, A. M. (2017). Role of pattern recognition receptors in the modulation of antimicrobial peptide expression in the corneal epithelial innate response to *F. solani*. *Invest. Ophthalmol. Vis. Sci.* 58, 2463–2472. doi: 10.1167/iovs.16.20658
- Laanto, E., Bamford, J. K., and Laakso, J. (2012). Phage-driven loss of virulence in a fish pathogenic bacterium. *PLoS One* 7:e53157. doi: 10.1371/journal.pone.0053157
- Li, L., Murdock, G., and Bagley, D. (2010). Genetic dissection of a mitochondria-vacuole signaling pathway in yeast reveals a link between chronic oxidative stress and vacuolar iron transport. *J. Biol. Chem.* 285, 10232–10242. doi: 10.1074/jbc.M109.096859
- Lin, L., Cao, J., Du, A., An, Q., Chen, X., Yuan, S., et al. (2021). eIF3k domain-containing protein regulates Conidiogenesis, Appressorium turgor, virulence, stress tolerance, and physiological and pathogenic development of *Magnaporthe oryzae*. *Front. Plant Sci.* 12:748120. doi: 10.3389/fpls.2021.748120
- Livak, K. J., and Schmittgen, T. D. (2001). Analysis of relative gene expression data using real-time quantitative PCR and the 2(-Delta Delta C(T)) method. *Methods* 25, 402–408. doi: 10.1006/meth.2001.1262
- Lorenzini, M., and Zapparoli, G. (2019). Yeast-like fungi and yeasts in withered grape carposphere: characterization of *Aureobasidium pullulans* population and species diversity. *Int. J. Food Microbiol.* 289, 223–230. doi: 10.1016/j.ijfoodmicro.2018.10.023
- Matsumoto, K., Ikema, K., and Tanihara, H. (2005). Role of cytokines and chemokines in pseudomonal keratitis. *Cornea* 24, S43–S49. doi: 10.1097/01.icc.0000178737.35297.d4
- Melotto, M., Brandl, M. T., Jacob, C., Jay-Russell, M. T., Micallef, S. A., Warburton, M. L., et al. (2020). Breeding crops for enhanced food safety. *Front. Plant Sci.* 11:428. doi: 10.3389/fpls.2020.00428
- Muraosa, Y., Oguchi, M., Yahiro, M., Watanabe, A., Yaguchi, T., and Kamei, K. (2017). Epidemiological study of fusarium species causing invasive and superficial Fusariosis in Japan. *Med. Mycol.* 58, E5–E13. doi: 10.3314/mmj.16-00024
- Nucci, M., and Anaissie, E. (2007). Fusarium infections in immunocompromised patients. *Clin. Microbiol. Rev.* 20, 695–704. doi: 10.1128/cmr.00014-07
- Paisley, D., Robson, G. D., and Denning, D. W. (2005). Correlation between in vitro growth rate and in vivo virulence in *Aspergillus fumigatus*. *Med. Mycol.* 43, 397–401. doi: 10.1080/13693780400005866
- Park, Y., Cho, Y., Lee, Y. H., Lee, Y. W., and Rhee, S. (2016). Crystal structure and functional analysis of isocitrate lyases from *Magnaporthe oryzae* and *Fusarium graminearum*. *J. Struct. Biol.* 194, 395–403. doi: 10.1016/j.jsb.2016.03.019
- Pranavathiyan, G., Prava, J., Rajeev, A. C., and Pan, A. (2020). Novel target exploration from hypothetical proteins of *Klebsiella pneumoniae* MGH 78578 reveals a protein involved in host-pathogen interaction. *Front. Cell. Infect. Microbiol.* 10:109. doi: 10.3389/fcimb.2020.00109
- Roth, M. G., and Chilvers, M. I. (2019). A protoplast generation and transformation method for soybean sudden death syndrome causal agents fusarium virguliforme and F. brasiliense. *Fungal Biol. Biotechnol.* 67. doi: 10.1186/s40694-019-0070-0
- Safavi, S. A., Shah, F. A., Pakdel, A. K., Reza Rasoulian, G., Bandani, A. R., and Butt, T. M. (2007). Effect of nutrition on growth and virulence of the entomopathogenic fungus *Beauveria bassiana*. *FEMS Microbiol. Lett.* 270, 116–123. doi: 10.1111/j.1574-6968.2007.00666.x
- Schmidpeter, J., Dahl, M., Hofmann, J., and Koch, C. (2017). ChMob2 binds to ChCbk1 and promotes virulence and conidiation of the fungal pathogen *Colletotrichum higginsianum*. *BMC Microbiol.* 17:22. doi: 10.1186/s12866-017-0932-7
- Selinski, J., and Scheibe, R. (2014). Pollen tube growth: where does the energy come from? *Plant Signal. Behav.* 9:e977200. doi: 10.4161/15592324.2014.977200
- Seok, H. Y., Kim, T., Lee, S. Y., and Moon, Y. H. (2022). Non-TZF transcriptional activator AtC3H12 negatively affects seed germination and seedling development in Arabidopsis. *Int. J. Mol. Sci.* 23:1572. doi: 10.3390/ijms23031572
- Uddin, R., Siddiqui, Q. N., Sufian, M., Azam, S. S., and Wadood, A. (2019). Proteome-wide subtractive approach to prioritize a hypothetical protein of XDR-mycobacterium tuberculosis as potential drug target. *Genes Genomics* 41, 1281–1292. doi: 10.1007/s13258-019-00857-z
- Vico, S. H., Prieto, D., Monge, R. A., Román, E., and Pla, J. (2021). The Glyoxylate cycle is involved in white-opaque switching in *Candida albicans*. *J. Fungi* 7:502. doi: 10.3390/jof7070502
- Wang, L., Chen, J., Zhao, Y., Wang, S., and Yuan, M. (2022). OsMAPK6 phosphorylates a zinc finger protein OsLIC to promote downstream OsWRKY30 for rice resistance to bacterial blight and leaf streak. *J. Integr. Plant Biol.* 64, 1116–1130. doi: 10.1111/jipb.13249
- Wang, B., Fang, R., Chen, F., Han, J., Liu, Y. G., Chen, L., et al. (2020). A novel CCCH-type zinc finger protein SAW1 activates OsGA20ox3 to regulate gibberellin homeostasis and anther development in rice. *J. Integr. Plant Biol.* 62, 1594–1606. doi: 10.1111/jipb.12924
- Wang, H. C., Ko, T. P., Wu, M. L., Ku, S. C., Wu, H. J., and Wang, A. H. (2012). Neisseria conserved protein DMP19 is a DNA mimic protein that prevents DNA binding to a hypothetical nitrogen-response transcription factor. *Nucleic Acids Res.* 40, 5718–5730. doi: 10.1093/nar/gks177
- Wang, L. L., Lee, K. T., Jung, K. W., Lee, D. G., and Bahn, Y. S. (2018). The novel microtubule-associated CAP-glycine protein Cgp1 governs growth, differentiation, and virulence of *Cryptococcus neoformans*. *Virulence* 9, 566–584. doi: 10.1080/21505594.2017.1423189
- Wang, C., Wang, Y., Zhang, L., Yin, Z., Liang, Y., Chen, L., et al. (2021). The Golgin protein RUD3 regulates *Fusarium graminearum* growth and virulence. *Appl. Environ. Microbiol.* 87, e02522–e02520. doi: 10.1128/AEM.02522-20
- Wei, Y., He, D., Zhao, B., Liu, Y., Gao, S., Zhang, X., et al. (2022). The sat1 gene is required for the growth and virulence of the human pathogenic fungus *aspergillus fumigatus*. *Microbiol. Spectr.* 10:e0155821. doi: 10.1128/spectrum.01558-21
- WHO (2022). WHO fungal priority pathogens list to guide research, development and public health action. Available at: <https://www.who.int/news/item/25-10-2022-who-releases-first-ever-list-of-health-threatening-fungi>
- Yi, D., Dempersmier, J. M., Nguyen, H. P., Viscarra, J. A., Dinh, J., Tabuchi, C., et al. (2019). Zc3h10 acts as a transcription factor and is phosphorylated to activate the thermogenic program. *Cell Rep.* 29, 2621–2633.e4. doi: 10.1016/j.celrep.2019.10.099
- Yu, Y., Zhong, J., Peng, L., Wang, B., Li, S., Huang, H., et al. (2017). Tacrolimus downregulates inflammation by regulating pro-/anti-inflammatory responses in LPS-induced keratitis. *Mol. Med. Rep.* 16, 5855–5862. doi: 10.3892/mmr.2017.7353
- Zhu, Y., Abdelraheem, A., Lujan, P., Idowu, J., Sullivan, P., Nichols, R., et al. (2021). Detection and characterization of fusarium wilt (*Fusarium oxysporum* f. sp. vasinfectum) race 4 causing fusarium wilt of cotton seedlings in New Mexico. *Plant Dis.* 105, 3353–3367. doi: 10.1094/PDIS-10-20-2174-RE
- Zou, Q., Gang, K., Yang, Q., Liu, X., Tang, X., Lu, H., et al. (2018). The CCCH-type zinc finger transcription factor Zc3h8 represses NF- $\kappa$ B-mediated inflammation in digestive organs in zebrafish. *J. Biol. Chem.* 293, 11971–11983. doi: 10.1074/jbc.M117.802975